Microbial Cell Factories

RESEARCH

Open Access

# Characterization of GQA as a novel β-lactamase inhibitor of CTX-M-15 and KPC-2 enzymes

Lamiaa A. Al-Madboly[1*], Mohamed A. Abd El-Salam[2,3*], Jairo K. Bastos[4], Shaimaa Aboukhatwa[5] and Rasha M. El-Morsi[6]

## Abstract

β-lactam resistance is a significant global public health issue. Outbreaks of bacteria resistant to extended-spectrum β-lactams and carbapenems are serious health concerns that not only complicate medical care but also impact patient outcomes. The primary objective of this work was to express and purify two soluble recombinant representative serine β-lactamases using *Escherichia coli* strain as an expression host and pET101/D as a cloning vector. Furthermore, a second objective was to evaluate the potential, innovative, and safe use of galloylquinic acid (GQA) from *Copaifera lucens* as a potential β-lactamase inhibitor.

In the present study, $bla_{CTX\text{-}M\text{-}15}$ and $bla_{KPC\text{-}2}$ represented genes encoding for serine β-lactamases that were cloned from parent isolates of *E. coli* and *K. pneumoniae*, respectively, and expression as well as purification were performed. Moreover, susceptibility results demonstrated that recombinant cells became resistant to all test carbapenems (MICs; 64–128 µg/mL) and cephalosporins (MICs; 128–512 µg/mL). The MICs of the tested β-lactam antibiotics were determined in combination with 4 µg/mL of GQA, clavulanic acid, or tazobactam against *E. coli* strains expressing CTX-M-15 or KPC-2-β-lactamases. Interestingly, the combination with GQA resulted in an important reduction in the MIC values by 64–512-fold to the susceptible range with comparable results for other reference inhibitors. Additionally, the half-maximal inhibitory concentration of GQA was determined using nitrocefin as a β-lactamase substrate. Data showed that the test agent was similar to tazobactam as an efficient inhibitors of the test enzymes, recording smaller $IC_{50}$ values (CTX-M-15; 17.51 for tazobactam, 28.16 µg/mL for GQA however, KPC-2; 20.91 for tazobactam, 24.76 µg/mL for GQA) compared to clavulanic acid. Our work introduces GQA as a novel non-β-lactam inhibitor, which interacts with the crucial residues involved in β-lactam recognition and hydrolysis by non-covalent interactions, complementing the enzyme's active site. GQA markedly enhanced the potency of β-lactams against carbapenemase and extended-spectrum β-lactamase-producing strains, reducing the MICs of β-lactams to the susceptible range. The β-lactamase inhibitory activity of GQA makes it a promising lead molecule for the development of more potent β-lactamase inhibitors.

**Keywords** Carbapenemase, Extended-spectrum β-lactamases, Galloylquinic acid, β-lactamase inhibitor, *Escherichia coli*, *Klebsiella pneumoniae*

*Correspondence:
Lamiaa A. Al-Madboly
lamia.youssif@pharm.tanta.edu.eg
Mohamed A. Abd El-Salam
mohamed.abdelsalam@deltauniv.edu.eg; mohamedabdelsalam@rcsi.ie
Full list of author information is available at the end of the article

## Introduction

In the twenty-first century, antibiotics, particularly those from the β-lactam class, are considered the cornerstones of antibacterial chemotherapy. A large proportion of recent hospital prescriptions include β-lactam drugs. The four main chemical classes represented by the most prevalent β-lactam-containing substances are penicillins, cephalosporins, carbapenems, and monobactams [1].

Ambler's categorization of molecular structure [2] and Bush and Jacoby functional classification [3] have been used to categorize β-lactamases. The Ambler classification divides β-lactamases into four classes, A, B, C, and D, respectively, based on motifs made up of the main sequences that make up the protein molecules. β-lactamases of classes A, C, and D use serine as the enzyme active center, while those of class B use zinc, hence consisting of two major families: serine-β-lactamases (SBLs) and Metallo-β-lactamases (MBLs). On the other hand, Bush and Jacoby functional classification divides β-lactamases into groups 1 through 3 based on how they break down β-lactam substrates and how inhibitors affect them [3].

Healthcare systems throughout the globe are threatened by emerging multi-drug resistance pathogens, especially when they cause hospital-acquired infections (HAIs). β-lactam resistance is considered a worldwide public health problem [5]. Extended-spectrum β-lactam- and carbapenem-resistant bacterial outbreaks are severe issues that not only make treatment challenging but also affect the prognosis of sick individuals [6].

One of the most important mechanisms of resistance exerted by bacteria against β-lactam antibiotics is the production of the β-lactam hydrolyzing enzyme, one essential example of β-lactamase enzyme is class A CTX-M β-lactamases, which were given their name because of their high activity against cefotaxime and other oxyimino β-lactam substrates like ceftazidime, ceftriaxone, and cefepime [7]. Numerous publications have demonstrated the involvement of CTX-M-type ESBL-producing strains in severe infections in both hospitalized and nonhospitalized individuals. It has been observed that the frequency of enzymes of the CTX-M type group is rising, particularly in *E. coli*. Furthermore, throughout the past 10 years, ESBLs of the CTX-M type have arisen in several nations worldwide [8]. Another important example is *Klebsiella pneumoniae* carbapenemase (KPC), which belongs to class A. *Klebsiella pneumoniae* carbapenemase (KPC) has been shown to have carbapenemase activity in both pathogenic and environmental organisms. β-lactam antibiotic family, which includes carbapenem, is an effective treatment for severe infections caused by *Pseudomonas aeruginosa, Klebsiella pneumoniae*, and other Gram-negative bacterial pathogens. Therefore, the development of resistance to this class of antibiotics is a significant concern. Carbapenems were formerly used as a last resort after all other treatment options had been exhausted. However, due to increasing resistance to other β-lactam families, such as cephalosporins and penicillins, the use of carbapenems to treat clinical infections is growing in popularity [9].

Gram-negative bacteria that produce β-lactamases have been classified by both the Centers for Disease Control and Prevention (CDC) and the World Health Organization (WHO) as among the world's most serious or critical risks [4]. There are few options for treating carbapenem-resistant-related infections, and these illnesses have high rates of clinical failure, morbidity, and mortality, particularly in patients receiving intensive care unit (ICU) care [10, 11].

New β-lactamase inhibitor (BLI) combinations represent substantial advancements in treating serious drug-resistant Gram-negative bacterial infections, moving away from old BLI combinations like amoxicillin/clavulanic acid, ampicillin/sulbactam, and piperacillin/tazobactam. Ceftolozane-tazobactam, ceftazidime-avibactam, meropenem-vaborbactam, and imipenem-sulbactam are four β-lactam-BLI combination medicines that were recently approved by the FDA [12].

*Copaifera* species, belonging to the family *Fabaceae*, include; *C. lucens* and *C. langsdorffii* which are common trees in Brazil known to have various promising biological activities, primarily their practice in the modulation of urolithiasis due to the presence of galloylquinic acid (GQA) in high percentage, representing the main secondary metabolite in the extract of the leaves. Additionally, galloylquinic acid was previously purified and identified by our co-workers using HPLC–UV analysis [13].

Methyl gallate and gallic acid both have enzyme-inhibitory activity related to the phenolic compounds' capacity to bind proteins. Moreover, penicillinase may be inhibited by epicatechin gallate, which has antibacterial action [14, 15]. Also, a recent study by Jiamboonsri et al. [16], reported that both methyl gallate and gallic acid possess a mild inhibitory effect on the β-lactamase enzyme. However, the combination of them with ampicillin was effective. So, they could work in conjunction with β-lactam antibiotics to treat MRSA infection.

These previous reports encourage us to test the enzyme inhibitory effect of the galloylquinic acid (GQA) compound. Therefore, our study aims to express and purify both CTX-M-15 and KPC-2 as well as explore the potential use of GQA as a novel β-lactamase inhibitor.

## Results

The minimum inhibitory concentrations (MICs) of several β-lactam antibiotics were determined against the test isolates using the broth microdilution assay, as shown in Table 1. Overall, the susceptibility test results revealed high MIC values against the test isolates, particularly for meropenem and cefalexin. *E. coli* and *K. pneumoniae* isolates demonstrated a broader range of MIC values (16 to 128 µg/mL and 8 to 256 µg/mL) when assessed for susceptibility to cefepime and ertapenem, respectively. Additionally, cefepime and ertapenem recorded $MIC_{90}$ of 32 µg/mL against both *E. coli* and *K. pneumoniae* isolates, respectively. Intrinsic antibacterial activity was exhibited by GQA alone against both test isolates, as presented in Table 1. However, the MIC values recorded against *E. coli* were lower than those of *K. pneumoniae*.

The test isolates were screened for the presence of $bla_{CTX\text{-}M\text{-}15}$ and $bla_{KPC\text{-}2}$ genes using the PCR technique. The data revealed that 16% and 24% of *K. pneumoniae* and *E. coli* isolates, respectively, harbored these genes. Additionally, the activity of β-lactamases in the crude extract was determined for positive isolates spectrophotometrically (Figure S1) and two of the highest β-lactamase producing isolates were selected for the cloning experiment. Their nucleotide sequences were examined for similarity in the GenBank database and deposited under accession numbers OQ579151 and OQ579150 for *CTX-M-15* and *KPC-2*, respectively. Also, Figure S2 showed the phylogenetic trees generated using COBALT tool and data regarding GQA cytotoxicity presented in Figure S3 that showed an $IC_{50}$ of 168.17 mg/mL on Vero cell line.

**Table 1** Range of minimum inhibitory concentrations (MICs) and $MIC_{90}$ of various β-lactam antibiotics and GQA was determined against different clinical isolates of *E. coli* and *K. pneumoniae*

| Antibiotics or GQA | MIC (µg/mL) * | | | |
|---|---|---|---|---|
| | *E. coli* | | *K. pneumoniae* | |
| | MIC range | $MIC_{90}$ | MIC range | $MIC_{90}$ |
| Meropenem | – | – | 128–1024 | 1024 |
| Imipenem | – | – | 64–512 | 256 |
| Ertapenem | – | – | 8–256 | 32 |
| Cefalexin | 512–1024 | 512 | – | – |
| Cefotaxime | 64–128 | 64 | – | – |
| Cefepime | 16–128 | 32 | – | – |
| GQA | 256–512 | 256 | 512–1024 | 256 |

* Breakpoints of meropenem 8 µg/mL; imipenem 4 µg/mL; ertapenem 0.5 µg/mL; cefalexin16 µg/mL; cefotaxime 2 µg/mL; cefepime 4 µg/mL according to EUCAST, 2024. This test was done against 50 isolates of *E. coli* and *K. pneumoniae*, 25 isolates for each

Tables 2 and 3 present the types of β-lactamases tested and the MIC values of β-lactam antibiotics in the absence and presence of GQA and other β-lactamase inhibitors. The results showed that GQA reduced the MIC values of all tested β-lactam antibiotics to the susceptible range against both isogenic strains producing CTX-M-15 and KPC-2 β-lactamases. For cefalexin, a dramatic reduction in the MIC was noticed (4 µg/mL; 128-fold reduction) after combining GQA with the test antibiotic (Table 2). Additionally, FICI values confirmed the synergistic effect ($FICI \leq 0.5$) of GQA/β-lactam combination. Results were comparable to both tazobactam and clavulanic acid combinations with the test antibiotics (Table 2). For all tested carbapenems, the MIC values showed 64-512-fold reductions following incubation of the KPC-2 producing isogenic strain in the presence of GQA (4 µg/mL)/carbapenem combination, as shown in Table 3. Interestingly, the MICs were markedly reduced below EUCAST breakpoints. To support the MIC results, a disc diffusion test was performed. Interestingly, enhanced clear inhibition zones were detected after adding 4 µg/mL of GQA to either cefotaxime or imipenem discs compared to the antibiotic discs only or even after adding low concentration of GQA (2 µg/mL) where growth of mutants inside the inhibition zones was detected, as shown in Fig. 1.

Figure 2 shows time-kill curves that evaluated the impact of GQA on the viable count of isogenic strains producing CTX-M-15 and KPC-2. Single drug tests did not result in a significant increase in the biomass of the test strains compared to the control. However, double combinations of antibiotics with either tazobactam or clavulanic acid demonstrated reductions in the viable count. The combination of cefotaxime with tazobactam resulted in viable count below the limit of detection after 6 h of incubation, however, GQA revealed the similar result after 8 h of incubation followed by clavulanic acid (10 h) as presented in Fig. 2A. Also, the combination of imipenem/clavulanic acid resulted in a 2-$log_{10}$ reduction in CFU after 6 h of incubation. However, a highly significant reduction ($p < 0.001$; ~ 5-$log_{10}$) was observed when GQA was combined with imipenem, indicating that GQA was more effective than clavulanic acid but similar in its activity to tazobactam (Fig. 2B). Interestingly, both tazobactam and GQA showed viable count below the limit of detection after 8 h of incubation.

Figure 3 shows the activities of CTX-M-15 and KPC-2, which were quantitatively determined in the presence or absence of GQA or other inhibitors using a spectrophotometric method. The data showed that tazobactam followed by GQA were superior in their effects on the test enzymes, recording relatively small $IC_{50}$ values (CTX-M-15; 17.51 & 28.16 µg/mL, KPC-2; 20.91 & 24.76 µg/mL, respectively) relative to clavulanic acid, as shown

**Table 2** The MIC values of cefalexin, cefotaxime, and cefepime alone and in combination with different inhibitors against engineered strains of *E. coli* producing CTX-M-15 cloned β-lactamase

| Isogenic Strains | Type of β-lactamase[a] | MIC data (μg/mL)[b] | | | | | | | | | | | |
|---|---|---|---|---|---|---|---|---|---|---|---|---|---|
| | | cefalexin | | | | cefotaxime | | | | cefepime | | | |
| | | Alone | with inhibitors | | | Alone | with inhibitors | | | Alone | with inhibitors | | |
| | | | GQA | Clav | Taz | | GQA | Clav | Taz | | GQA | Clav | Taz |
| BL10 (pUCP24 vector pET101/D-TOPO®) | – | 0.25 | 0.25 | 0.25 | 0.25 | 0.25 | 0.25 | 0.25 | 0.25 | 0.25 | 0.25 | 0.25 | 0.25 |
| TOP10-E375 | CTX-M-15 | 512 | 4 (0.50) | 8 (0.51) | 2 (0.50) | 128 | 0.5 (0.25) | 1 (0.26) | 0.25 (0.50) | 128 | 0.5 (0.25) | 1 (0.27) | 0.5 (0.25) |

[a] Type of β-lactamase was confirmed by both PCR using specific primers as well as sequencing

[b] *GQA* galloylquinic acid, *Clav* clavulanic acid, *Taz* tazobactam. All inhibitors were tested at a constant concentration of 4 μg/mL. FICI values are presented between brackets

**Table 3** The MIC values of carbapenems alone and in combination with different inhibitors against engineered strains of *E. coli* producing KPC-2 cloned β-lactamase

| Isogenic Strains | Type of β-lactamase[a] | MIC (μg/mL)[b] | | | | | | | | | | | |
|---|---|---|---|---|---|---|---|---|---|---|---|---|---|
| | | Ertapenem | | | | Meropenem | | | | Imipenem | | | |
| | | Alone | with inhibitors | | | Alone | with inhibitors | | | Alone | with inhibitors | | |
| | | | GQA | Clav | Taz | | GQA | Clav | Taz | | GQA | Clav | Taz |
| BL10 (pUCP24 vector pET101/D-TOPO®) | – | 0.25 | 0.25 | 0.25 | 0.25 | 0.25 | 0.25 | 0.25 | 0.25 | 0.25 | 0.25 | 0.25 | 0.25 |
| TOP10-K6 | KPC-2 | 128 | 0.25 (0.25) | 0.5 (0.25) | 0.25 (0.25) | 128 | 2 (0.25) | 4 (0.50) | 1 (0.50) | 64 | 1 (0.13) | 2 (0.50) | 1 (0.50) |

[a] Type of β-lactamase was confirmed by both PCR using specific primers as well as sequencing

[b] *GQA* galloylquinic acid, *Clav* clavulanic acid, *Taz* tazobactam. All inhibitors were tested at a constant concentration of 4 μg/mL. FICI values are presented between brackets

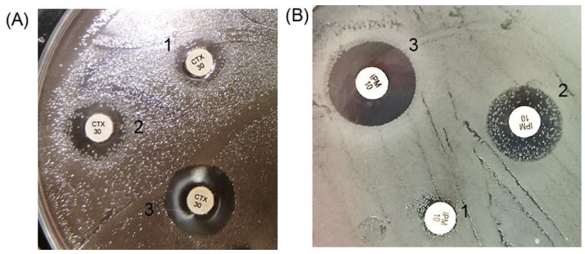


**Fig. 1** Effect of different concentrations of GQA on the susceptibility of isogenic strains, namely CTX-M-15-producer (**A**) to cefotaxime (CTX) disc and KPC-2-producer (**B**) to imipenem (IPM) disc. A1: CTX disc only showing resistance. A2: CTX disc to which 2 µg/mL of GQA was added showing an inhibition zone with some mutants. A3: CTX disc to which 4 µg/mL of GQA was added showing with an enhanced clear inhibition zone. B1: IPM disc only showing resistance. B2: IPM disc to which 2 µg/mL of GQA was added showing an inhibition zone with a lot of mutants. B3: IPM disc to which 4 µg/mL of GQA was added showing an enhanced clear inhibition zone

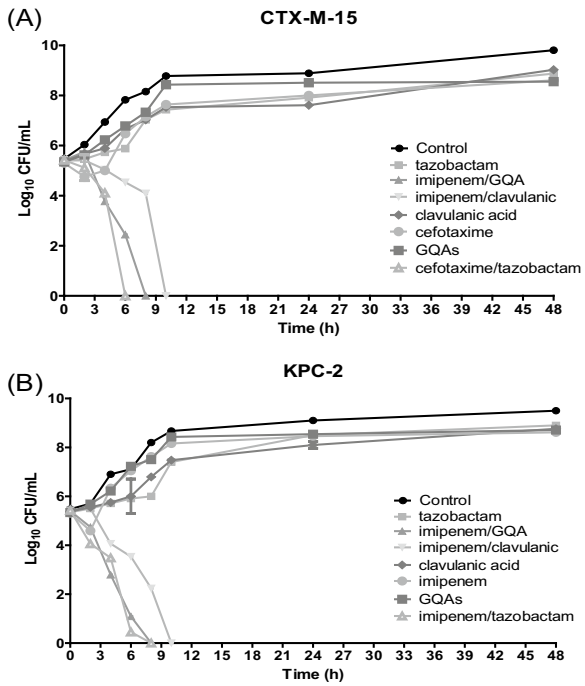


**Fig. 2** Evaluation of combining 4 µg/mL of GQA with 2 µg/mL of cefotaxime as a cephalosporin (**A**) or 4 µg/mL of imipenem as a carbapenem (**B**) against isogenic strains producing the test β-lactamase. Other reference inhibitors, such as clavulanic acid or tazobactam, were also assessed at a fixed concentration of 4 µg/mL. Concentrations of antibiotics represented their breakpoint according to EUCAST guidelines (2024)

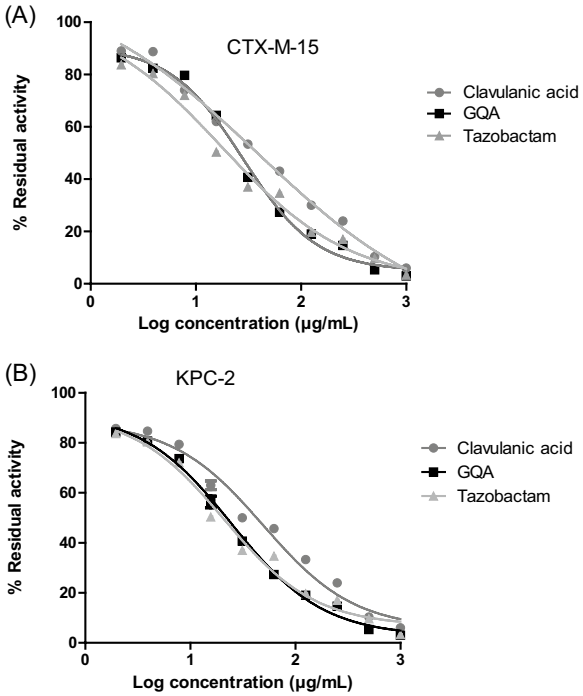


**Fig. 3** Representation of the half maximal inhibitory concentration ($IC_{50}$) values for GQAs, clavulanic acid, and tazobactam against the CTX-M-15 (**A**) and KPC-2 (**B**) enzymes are shown as percent residual activity of the test enzyme against log concentrations of the compounds and nitrocefin was used as a substrate. $IC_{50}$ calculated by GraphPad prism software

in Table 4. Furthermore, tazobactam showed the highest affinity for KPC-2 (29.16 µM) and closely followed by GQA (30 µM), however, both tazobactam and GQA approximately recorded the same affinity to CTX-M-15 with $K_i$ value of ~ 31 µM as presented in Table 4.

The hydrolysis of different nitrocefin concentrations by either CTX-M-15 or KPC-2 in the absence or presence of 4 µg/mL of GQA was performed. Data were presented as Lineweaver–Burk plot as shown in Fig. 4. The $K_m$ values of nitrocefin hydrolysis was found to be low (high affinity) in the absence of the test inhibitor while values were found to be increased in the presence of GQA indicating that the affinity was reduced. Moreover, the $V_{max}$ value did not change for each enzyme denoting that GQA inhibited both enzymes via reversible competitive inhibition (Fig. 4).

Regarding Docking data, the predicted interaction mode of GQA with CTX-M-15 is provided in Fig. 5. The active site pocket of CTX-M-15 was defined by a bound boronic acid inhibitor ligand in the X-ray crystal structure (PDB: 5T66). The model predicts multiple hydrogen bonding and van der Waals interactions between the active site residues and the ligand (Fig. 5A). The phenolic OH groups on the galloyl moieties hydrogen bond with Glu274, Lys272, Pro170, Ser133 and Asn135. The

**Table 4** $IC_{50}$ and $K_i$ regression results of GQA in µg/mL and µM, respectively, compared to other inhibitors

| Test enzyme | Parameter | Tazobactam | GQA | Clavulanic acid |
|---|---|---|---|---|
| CTX-M-15 | $IC_{50}$ | 17.51 | 28.16 | 38.99 |
| | $K_i$ | 31.22 | 31.00 | 33.43 |
| KPC-2 | $IC_{50}$ | 20.91 | 24.76 | 49.54 |
| | $K_i$ | 29.16 | 30.00 | 32.20 |

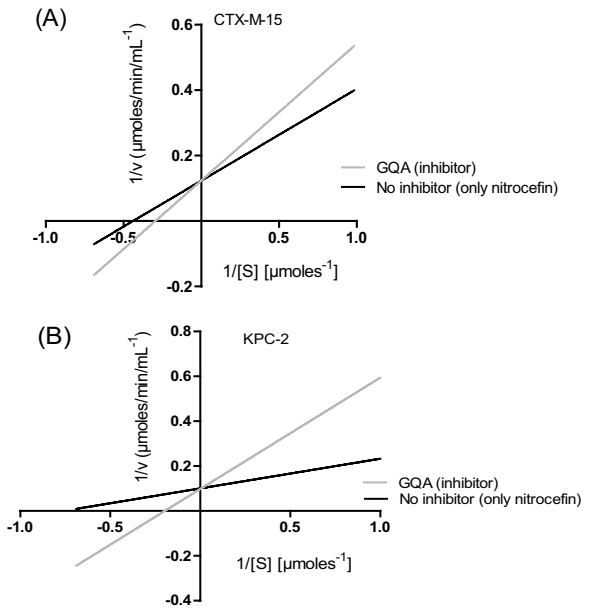


**Fig. 4** Lineweaver–Burk plot showing the mechanism through which GQA hinders CTX-M-15 (**A**) and KPC-2 (**B**), via monitoring the hydrolysis of various nitrocefin concentrations using the test enzyme in the presence of 4 µg/mL of GQA

cyclohexyl-1-carboxylate anion in the top scoring pose forms a hydrogen bond with Ser275 (Fig. 5B). Several other solvent water molecules mediated hydrogen bonding interactions were observed, and are not shown in the figure for clarity.

The predicted interaction mode of GQA with KPC-2 is shown in Fig. 5. The active site pocket of KPC-2 as defined by the bound ligand in the X-ray crystal structure (PDB: 6QW9), shows a highly ionizable surface with both basic and acidic Electrostatic surface potential (ESP) regions (Fig. 6A). The GQA compound docking pose with KPC-2 shows a network of hydrogen bonds of the active site amino acids with the 1-carboxylic acid group on the central cyclohexane and the phenolic OH groups on the 3- and the 5-trihydroxybenzoyl moieties (Fig. 6A). The 4-trihydroxybenzoyl group was directed towards the enzyme solvent accessible surface (Fig. 6A). The cyclohexyl-1-carboxylate anion forms salt bridge and ionic bond with the cationic side chains of two basic amino acids; both Lys234 and Arg220. In addition, the carboxylate ($O^-$) acts as a hydrogen bond acceptor with both Ser130 and Thr235. The carbonyl oxygen (C=O) accepts a hydrogen bond from Thr237 (Fig. 6B). The molecule is firmly anchored in the active site pocket by a vast network of advantageous interactions. Additional hydrogen bonds are formed between the side chains of Thr215, Asn132, Asn170, and Glu166 and the phenolic groups of the 3- and 5-galloyl portions. Two more van der Waals contacts were noted: the π-σ interaction between Thr216 and the 5-galloyl group's phenyl ring, and the π-π stacking interaction between Trp105 and the 3-galloyl group's phenyl ring (Fig. 6B). Several additional solvent water molecules were found to facilitate hydrogen bonding interactions, the most significant of which included the nucleophilic Ser70 in the active site. For clarity, these are not displayed in the figure.

## Discussion

Antibiotics are commonly used to treat bacterial infections in human medicine. However, the effectiveness of these drugs has become inadequate due to the continuous development of antibiotic resistance, which is a worldwide health problem with a significant economic and social impact [17]. Resistance to β-lactam antibiotics, particularly cephalosporins and penicillins, which are extensively used categories of antibiotics, is a significant problem that requires immediate attention. This resistance is caused by many factors, including: (i) modification of porin channels through which antibiotics diffuse, (ii) mutations in the target, such as penicillin-binding proteins involved in cell wall biosynthesis, (iii) overexpression of efflux pumps that lead to the export of antibiotics outside bacterial cells, and most importantly, (iv) expression of β-lactamases that hydrolyze the β-lactam ring of antibiotics, thus rendering them inactive [18–22].

CTX-M-15 is a widely disseminated extended-spectrum β-lactamase in community settings and hospitals. It is highly active on cephalosporins particularly, cefotaxime and ceftazidime due to selective pressure on these antibiotics [23, 24]. In the present work, genotypic detection of $bla_{CTX\text{-}M\text{-}15}$ gene was performed and positive isolates were subjected to phenotypic confirmation by β-lactamase assay based on nitrocefin as a substrate. A strong β-lactamase producing isolate was selected and used for cloning.

An *Escherichia coli* clinical isolate $bla_{CTX\text{-}M\text{-}15}$ gene was cloned, produced, and the CTX-M-15 protein was purified. According to Faheem et al. [17], a single protein band with a molecular weight of 31 kDa was observed in the stained gel after PAGE when compared to the unpurified lane, indicating more than 95% purity. Furthermore,

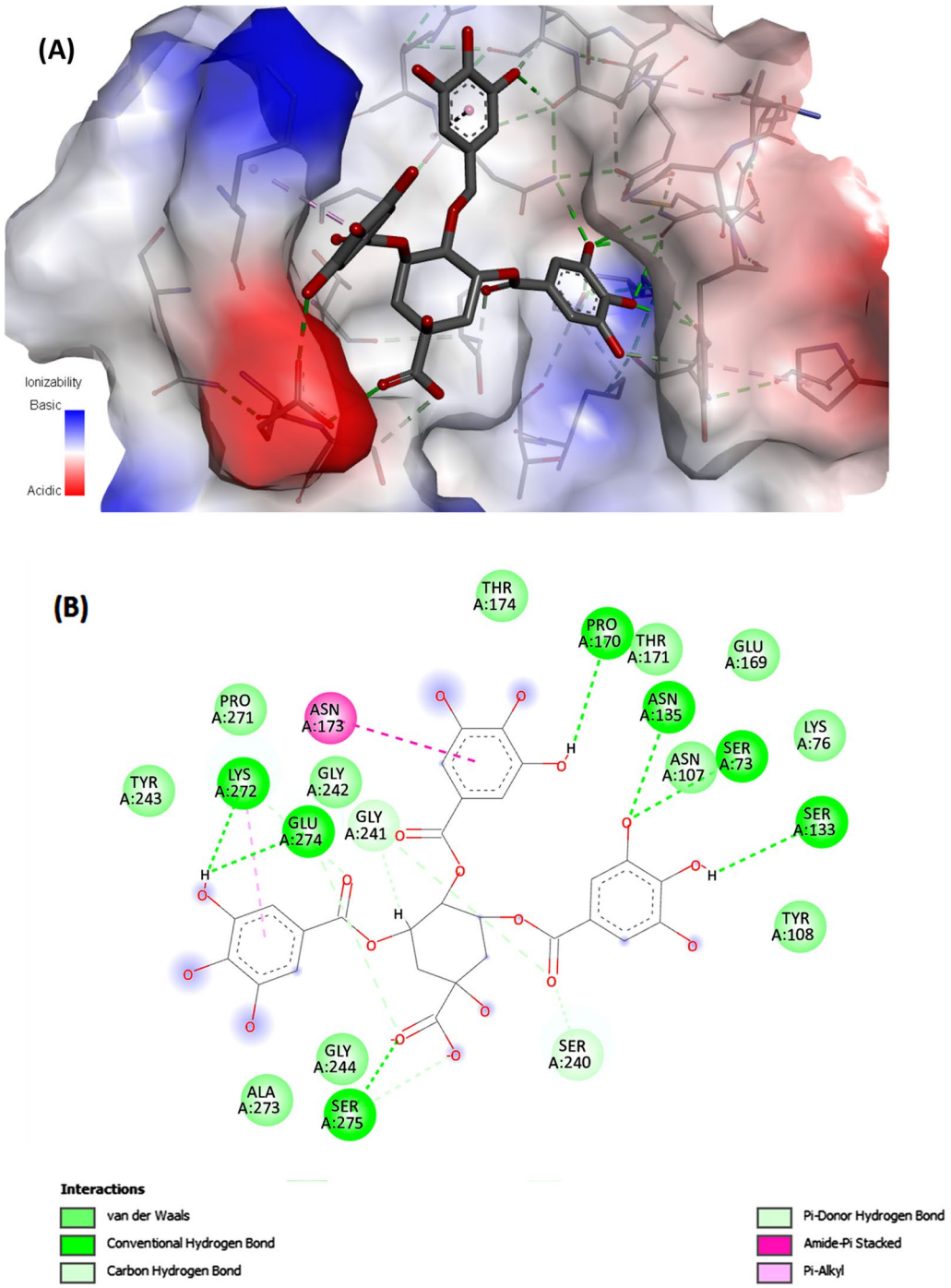


**Fig. 5** **A** Predicted binding mode of LM to the active site of CTX-M-15 (PDB: 5T66). The ligand (GQAs) is shown as CPK-colored thick sticks. The amino acids in the active site are shown as sticks. Electrostatic surface potential (ESP) of the protein active site is shown; Red represents negatively charged (acidic) ESP and Blue is for positive (basic) ESP. Green dashed lines represents the hydrogen bonds between the ligand and the protein MOE Docking score (S Score) of the pose selected = – 7.8 kcal/mol. **B** 2 D interaction diagram of interaction between GQAs and the active site amino acids of CTX-M-15 (PDB: 5T66). The solvent accessible surface is shown by light blue shades

in the presence and absence of GQA, the MICs of various cephalosporins were assessed on the transformant cloned with the $bla_{CTX\text{-}M\text{-}15}$ gene. Significant drops in the MICs were recorded (128–256-fold) when compared to the reference β-lactamase inhibitors, suggesting comparable potency. Furthermore, the development of mutants

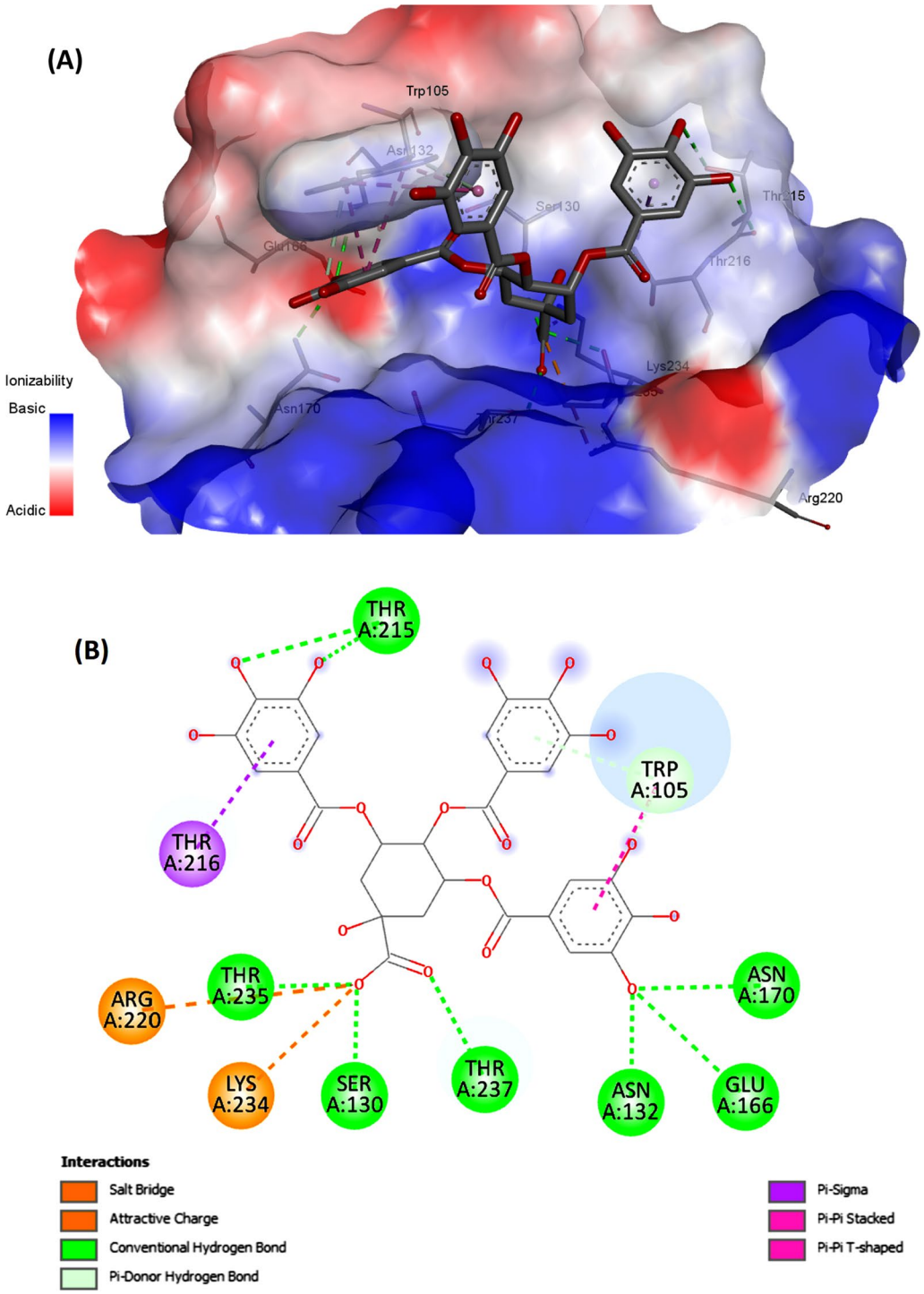


**Fig. 6** **A** Predicted binding mode of GQA to the active site of KPC-2 (PDB: 6QW9). The ligand (GQAs) is shown as CPK-colored thick sticks. The amino acids in the active site are shown as sticks. Electrostatic surface potential (ESP) of the protein active site is shown; Red represents negatively charged (acidic) ESP and Blue is for positive (basic) ESP. Green dashed lines represents the hydrogen bonds between the ligand and the protein MOE Docking score (S Score) of the pose selected = – 7.6 kcal/mol. **B** 2 D interaction diagram of interaction between LM and the active site amino acids of KPC-2 (PDB: 6QW9). The solvent accessible surface is shown by light blue shades

was suppressed by adding a sub-MIC of GQA (4 µg/mL) to CTX discs. Faheem et al. [17] demonstrated that tazobactam decreased the MICs of some cephalosporin antibiotics to about 2–16 folds and also decreased in the presence of ZINC03787097 to the same level noticed in case of cephalosporin-sulbactam combination.

One major concern is the rapid development of carbapenemase-encoded resistance in Gram-negative bacterial pathogens, especially in *K. pneumoniae*, which puts the efficacy of approved carbapenems and their inhibitors at risk. These antibiotics are considered last-resort antimicrobials used to treat serious nosocomial infections [25]. Carbapenemases, or carbapenem-hydrolyzing β-lactamases, are a major cause of carbapenem resistance, especially *K. pneumoniae* carbapenemase-2 (KPC-2). In this study, the $bla_{KPC-2}$ gene was cloned from a parent isolate of *K. pneumoniae*, expressed, and purified, yielding a single 28 kDa protein band following PAGE. Susceptibility data showed that the recombinant cells were resistant to all tested carbapenems, recording high MICs (64–128 µg/mL). However, after combining with 4 µg/mL of GQA, the MIC values were dramatically reduced by 64–512-fold. Similar results were reported by Khan et al. [26], where ertapenem and meropenem showed an eightfold reduction in MIC values, and imipenem MIC was reduced by fourfold following combination with two new enzymatic inhibitors (ZINC01807204 and ZINC02318494). However, these inhibitors were unable to restore the activity of carbapenem as none of them changed the MIC to the susceptible range. This might be due to the outer membrane proteins, which are known to have a role in the development of resistance phenotype. On the other hand, GQA was able to reduce the carbapenem MICs to the susceptible range, indicating its superiority.

In our study, we found that GQA had a smaller $IC_{50}$ value (CTX-M-15; 28.16 and KPC-2; 24.76 µg/mL) as an inhibitor on the test enzymes compared to both clavulanic acid and tazobactam, indicating similar efficiency. This suggests that GQA could be used as an alternative to traditional antibiotic-inhibitor combinations when combined with cephalosporin or carbapenem antibiotics. In addition, the demonstrated safety of GQA on Vero cells recorded an $IC_{50}$ of 168.17 mg/mL and this was also confirmed by Al-Madboly et al. [27]. Interestingly, this is the first study showing the effectiveness of GQA as a β-lactamase inhibitor against both CTX-M-15 and KPC-2, in comparison to traditional β-lactamase inhibitors such as clavulanic acid and tazobactam. Moreover, these findings were supported by the docking results in our work that showed extensive network of favorable interactions between both GQA and test enzymes. Faheem et al. [17] and Barnes et al. [28] reported similar results.

In conclusion, our work demonstrates that GQA could be considered as a novel non-β-lactam inhibitor that complements the enzymatic active site and hence interacted with the crucial residues involved in the recognition of β-lactam ring and its hydrolysis. Unlike conventional β-lactamase inhibitors, GQA could bind to the active site via non-covalent interactions including; hydrophobic interactions and hydrogen bonding. The advantage of using GQA is that MICs of test antibiotics reduced to the susceptible range. Lastly, our data concerning the promising MICs (after combinations) as well as the $IC_{50}$ values denoted that GQA test agent is an appropriate lead molecule for developing β-lactamase inhibitors with more potent effect.

## Material and methods

### Materials

#### *Galloylquinic acid (GQA)*

The leaves of *Copaifera lucens* were obtained from the Rio de Janeiro botanical garden, Arboreto, Canteiro, Brazil, and identified by botanist Haroldo Cavalcante de Lima. A voucher sample (RB 474303) was reserved as a reference at the Pharmacognosy laboratory at FCFRP, Brazil. GQA was extracted, purified and identified spectrophotometrically from the *n*-butanolic fraction of *C. lucens* using HPLC, based on their characteristic UV spectra, as previously described in our studies [13, 29]. A stock solution (50 mg/mL) was prepared in dimethyl sulfoxide (DMSO) and stored at – 80 ℃ until use.

**Table 5** Test isolates and primer sequences used for cloning different β-lactamase genes via TOPO® cloning are listed

| Test isolate* | β-lactamase gene | Primer name | Primer sequence (5′ to 3′) | Annealing temp. (°C) |
|---|---|---|---|---|
| E343 | $bla_{CTX-M-15}$ | CTX-M-15-F | CACCGGAATCTGACGCTGGGTAAA | 64 |
| | | CTX-M-15-R | GGTTGAGGCTGGGTGAAGTA | |
| K14 | $bla_{KPC-2}$ | KPC-2-F | CACCCAGCTCATTCAAGGGCTTTC | 63 |
| | | KPC-2-R | GGCGGCGTTATCACTGTATT | |

* Abbreviations related to species served as a source of cloned genes: E, *E. coli;* K, *K. pneumoniae*. Design of primers and experimental procedures for "TOPO" cloning were carried out according to manufacturer's instructions provided with "Champion™ pET Directional TOPO® Expression" kit (Cat. no.; K101-01)

### *Antibiotics*

Dry powders of the following antibiotics were obtained from El-Borg Pharmaceutical Industry Company in Alexandria, Egypt: ertapenem, meropenem, imipenem, cefalexin, cefotaxime, and cefepime. Clavulanic acid was obtained as a gift from Amoun company for pharmaceutical drugs, while tazobactam was purchased from Sigma Aldrich, USA.

### Clinical isolates of *Bacteria*

A total of fifty clinical isolates of multidrug-resistant *E. coli* and *K. pneumoniae* were obtained from the Department of Microbiology and Immunology at the Faculty of Pharmacy, Tanta University, Egypt. These isolates were previously identified and tested for multiple drug resistance in studies conducted by Abdelaziz et al. [30] and Al-Madboly et al. [31].

### Susceptibility testing of clinical isolates

Susceptibility testing was conducted on clinical isolates by determining the minimum inhibitory concentrations of β-lactam antibiotics using the Mueller–Hinton broth microdilution assay in accordance with EUCAST [32] guidelines. Additionally, *E. coli* ATCC 25922 was used as a quality control strain.

### Polymerase chain reaction (PCR) technique

The polymerase chain reaction (PCR) technique was utilized to screen the test isolates for β-lactamase genes ($bla_{KPC-2}$ & $bla_{CTX-M-15}$) using primers designed in this study with primer3® (version 0.4.0). Table 5 provides the complete set of primers designed for amplification of the two β-lactamase genes. The amplification conditions were adjusted as follows: initial denaturation at 95 ℃ for 1 min, followed by 35 cycles of denaturation at 95 ℃ for 15 s, annealing for 15 s, and elongation at 72 ℃ for 30 s. Finally, PCR reactions were completed with a final elongation at 72 ℃ for 5 min. The annealing temperatures for each test gene are specified in Table 5. The PCR products were analyzed by agarose gel electrophoresis and cleaned using a PCR Clean Up kit (GeneDirex, Taiwan).

### Determination of β-lactamase enzymatic activity in crude extracts

Isolates that showed positive results in the PCR experiment were used to prepare cell-free extracts according to Shoeib et al. [33]. Quantitative determination of β-lactamase activity was performed using a β-lactamase activity assay kit (Sigma-Aldrich, USA). This test relies on the hydrolysis of nitrocefin, a non-antimicrobial cephalosporin, by the test enzyme, resulting in the production of a colorimetric product with an absorbance measured at 490 nm using a plate reader. One unit of β-lactamase activity is defined as the amount of enzyme required to hydrolyze 1.0 µmol of nitrocefin per minute at 25 ℃ and pH 7.0 [34].

### Construction of engineered bacterial strains with cloned β-lactamase gene

We used selected isolates of *E. coli* and *K. pneumoniae* that heavily produce KPC-2 and CTX-M-15 β-lactamases as parent strains. We amplified the test β-lactamase genes using PCR and used the resulting products to construct isogenic strains. These strains were then used to assess the enzyme inhibition profile by sub-MIC of GQAs and comparator β-lactamase inhibitors.

Briefly, clinical isolates producing different β-lactamases were used as DNA templates for PCR amplification using Xpert amplifi 2X high-fidelity DNA polymerase. The PCR primers were designed to contain CACC sequences to allow for cloning into the pET101/D-TOPO® vector (5753 nucleotides). Cloning was performed according to the manufacturer's instructions using One Shot® TOP10 *E. coli* strain. Plasmid DNA was then extracted and purified from the transformants, and PCR and sequencing were conducted to verify the presence of the target gene. A combination of reverse and forward sequencing primers, along with a primer that could hybridize within the insert, were used for PCR amplification.

The sequences were screened using the VecScreen tool (https://www.ncbi.nlm.nih.gov/tools/vecscreen/) to identify the presence of vector sequences. The vector sequences were then removed using (R 4.2.1, script), resulting in pure gene sequences. The pure gene sequences were deposited in GenBank, and accession numbers were provided. Phylogenetic trees were generated using the Constraint-Based multiple Alignment Tool (COBALT) (https://www.ncbi.nlm.nih.gov/tools/cobalt/re_cobalt.cgi).

### Expression of β-lactamases in engineered bacterial strains containing cloned genes

For the expression experiment, the BL21 Star™(DE3) One Shot chemically competent *E. coli* strain was transformed with the Champion™ pET Directional TOPO® Expression kit (Cat. # 101–01, Invitrogen) to express T7-regulated genes. Transformants were selected using LB agar supplemented with 100 µg/mL of ampicillin, and the appropriate pET TOPO® vector with the *lacZ* gene was used as a positive expression control in each Champion™ pET Directional TOPO® Expression kit.

β-lactamase test genes were expressed following the manufacturer's instructions. Briefly, transformants were grown in Luria Bertani broth (LB) containing 100 µg/mL of ampicillin and incubated at 31 ± 1 ℃ with shaking until

the optical density reached OD600 0.6. Gene expression was induced by adding 0.5 mM IPTG (isopropyl-D-thiogalactopyranoside), and cells were allowed to grow for 3 h. Bacterial cells were harvested by centrifugation at 8000 rpm for 10 min, and each pellet was resuspended in 20 mL of lysis buffer (300 mM NaCl, 50 mM Tris, pH 8.0, and 0.1% β-mercaptoethanol). Cells were ruptured by sonication on ice with 25 pulses alternating with 10 s at 30% amplitude. Cellular debris was separated by centrifugation at 12,000 rpm for 30 min. The Pierce™ Ni–NTA Purification System (Thermo Scientific, Germany) was used to purify the enzymes according to the manufacturer's instructions. The pure proteins were obtained by dialyzing the eluted fractions against 50 mM phosphate buffer (pH 8.0) with 100 mM sodium chloride. Purity was checked and evaluated using SDS-PAGE, and gels were stained with CBB-R250. Also, purity was confirmed by MALDI-TOF MS [17, 26].

#### Cytotoxicity assessment of GQA

The MTT assay was followed to test the safety of GQA on normal Vero cell line using a concentration range of 13.875 to 222 mg/mL as previously described by Ribeiro et al. [35].

#### Antibiotic susceptibility testing of recombinant *E. coli* strains

Recombinant *E. coli* BL21 cells harboring β-lactamase genes were tested for antibiotic susceptibility using a microdilution assay to determine the MIC of various β-lactams alone and in combination with test inhibitors (GQA, tazobactam or clavulanic acid) compared to control cells of BL21 with null vector. Before the experiment, the recombinant cells were induced with IPTG. The β-lactam antibiotics were tested according to EUCAST guidelines [32], with solutions added to microtiter plates followed by serial two-fold dilutions. Each inhibitor was evaluated at a fixed concentration of 4 µg/mL. Planktonic cultures of the test strains were grown overnight in LB broth at 37 ℃, adjusted with double-concentrated Mueller–Hinton broth to a final inoculum of $5\times10^5$ CFU/mL. Plates were then incubated at 37 ℃ for 24 h, and results were interpreted according to EUCAST guidelines [32]. The MIC was defined as the lowest concentration that completely inhibited visible bacterial growth. The fractional inhibitory concentration index (FICI) was determined according to the following equation:

$$FICI_{A/B} = MIC_A(\text{combination})/MIC_A(\text{alone}) + MIC_B(\text{combination})/MIC_B(\text{alone})$$

The interpretation of FICI was carried out according to Zhou et al. [36] and Al-Madboly [37] where FICI values of ≤ 0.5 indicate synergism, values between 0.5 and 4 indicate indifference or no interaction, while FICI values greater than 4 indicate antagonism.

#### Disc diffusion test

This was performed as described by Al-Madboly [22] and EUCAST guidelines [32] for assessment of the antimicrobial susceptibility in the absence or presence of 2 or 4 µg/mL of GQA. Briefly, 0.5 McFarland of test bacterial suspension was dispersed along the surface of an appropriate medium (Mueller–Hinton) agar plates by a cotton swab. The test antibiotic discs were placed on the surface of the medium as follows; three cefotaxime discs (30 µg; Oxoid) were transferred to the test plate where one disc was left as it is, however 2 or 4 µg/mL of GQA was added to the other two discs. Similarly, three imipenem discs (IPM-10 µg; Oxoid) were tested and all agar plates were incubated at 35 ± 1 ℃ for 18 ± 2 h. Following incubation, plates were examined for inhibition zones where zone edges were read as the point displaying no growth observed from the back of test plate in contrast to a dark background that was illuminated with reflected light.

#### Time-kill kinetic assay

A time-kill kinetic assay was used to evaluate the potential synergistic effect of GQA combined with test antibiotics to restore their activities, following the methodology described by Lagerback et al. [38] and Yang et al. [39]. Bacterial cells were diluted to a concentration of $5\times10^5$ CFU/mL and then incubated with 4 µg/mL of GQA and breakpoints of either cefotaxime (2 µg/mL) or imipenem (4 µg/mL). At specific time intervals (0, 2, 4, 6, 8, 10, 24, and 48 h), aliquots were taken to determine the viable count, which was plotted as time versus $\log_{10}$ CFU/mL. Other reference inhibitors (4 µg/mL of clavulanic acid or tazobactam) were also tested in the absence or presence of test antibiotics for comparison.

#### Purified β-lactamase enzymatic activity and inhibition assays

The activity of the purified β-lactamases was evaluated using a β-lactamase activity assay kit (Sigma-Aldrich, USA) as previously described by Everaert and Coenye [34].

### Determination of $IC_{50}$

The $IC_{50}$ value was determined using nitrocefin, a β-lactamase substrate, and inhibitors under controlled experiments. Purified β-lactamase enzyme was pre-incubated with different concentrations of GQA, clavulanic acid or tazobactam in 50 mM sodium phosphate buffer (PB, pH 7.0) at 30 ℃ for 5 min before the addition of the substrate; nitrocefin [17, 40]. The hydrolysis rate of nitrocefin was monitored by measuring the change in absorbance at 490 nm resulting from β-lactam ring cleavage using a TecanTM Sunrise plate reader (Austria). $IC_{50}$ values were determined by plotting the percentage residual enzyme activity exerted on nitrocefin against the concentration of the inhibitor using nonlinear regression and sigmoidal dose response analysis with PRISM 5.0 software (Graphpad Software, Inc., San Diego, CA). The $IC_{50}$ values, expressed in μM with 95% confidence intervals, were determined from at least three independent experiments, and the concentration of the test inhibitor that inhibited the enzyme's hydrolytic activity by 50% was considered the $IC_{50}$ value [26, 41, 42]. Data were shown as percent residual activity of the test enzyme against log concentrations of the compounds and nitrocefin was used as a substrate. $IC_{50}$ values were calculated using GraphPad prism software.

### Determination of the kinetic parameters

Purified β-lactamase enzymes were subjected to kinetic parameters measurements that were carried out in 100 mM sodium phosphate (pH 7.0) at 30 ℃ [17, 47]. This was determined spectrophotometrically via analysis of nitrocefin hydrolysis under initial-rate conditions.

### Mechanism of action of GQA

It was determined through monitoring the nitrocefin hydrolysis by CTX-M-15 as well as KPC-2 in the absence or presence of 4 μg/mL of GQA as described by Faheem et al. [17] with some modifications according to the manufacturer's instructions of the commercial kit used.

### Docking simulation of GQA compound to the β-lactamase CTX-M-15 and the carbapenemase KPC-2

#### *Background*

The compound of interest is a hydrolysable tannin with a 3,4,5-Tri-O-galloylquinic acid structure, previously demonstrated an increased susceptibility of MRSA to oxacillin [43, 44]. Both CTX-M-15 and KPC-2 are serine-based β-Lactamases.

#### *Docking simulation methods*

Molecular modeling studies were performed according to previously reported methodology [45, 46]. Docking simulation was performed using Molecular Operating Environment software (MOE version 2020, Chemical Computing Group Inc., Montreal, Canada) [47]. The selected pose in complex with the respective protein was imported in Biovia Discovery Studio Visualizer 2021, for visualization and generation of the interaction diagrams [48].

For CTX-M-15 docking, the X-ray diffraction crystal structure of a CTX-M-15 in complex with a cyclic boronate inhibitor, at a resolution of 1.95 Å, was downloaded from the RSCB-PDB (PDB ID: 5T66) [49].

For KPC-2 docking, the X-ray diffraction crystal structure of KPC-2 complexed with relebactam, at a resolution of 1.04 Å, was downloaded from the RSCB-PDB (PDB ID: 6QW9) [50].

In each case, the biological assembly was imported into the workspace of MOE. The structure preparation wizard of MOE was employed to correct the detected structural errors and to adjust the protonation state of the proteins via Protonate 3D, at 277 °K and pH 7.4. Partial charges were assigned using Merck Molecular Force Field 94x (MMFF94X) and hydrogen atoms were minimized [51]. The ligand-binding site was used as search space for potential docking poses. The energy of the complex was minimized using Amber10:EHT forcefield, which include parameters for proteins and small molecules, at a RMS gradient of 0.1 kcal/mol/ $Å^2$.

In order to evaluate the docking protocol for the purpose at hand, the active ligand in each case, was re-docked into the active site of the corresponding bound protein structure, using triangle matcher placement with London dG score and rigid receptor refinement with Generalized-Born Volume Integral/Weighted Surface area GBVI/WSA dG re-scoring function [52]. The RMSD after refinement for the returned poses of a cyclic boronate inhibitor in CTX-M-15 (PDB: 5T66) was 1.41 Å. The RMSD after refinement for the returned poses of relebactam in KPC-2 (PDB: 6QW9) was 1.6 Å.

Docking simulation used Triangle Matcher placement method and the docked poses were scored by the London dG scoring function. Docking poses were refined via rigid receptor refinement with Generalized-Born Volume Integral/Weighted Surface area GBVI/WSA dG re-scoring function.10 The energy of the protein–ligand complex was minimized at a RMS gradient of 0.1 kcal/mol/ $Å^2$, using Amber10:EHT forcefield, which include parameters for both proteins and small molecules. The returned poses in each docking experiment were visually inspected. The best pose was selected based on the highest score (S score) and the most favorable interactions formed with the critical active site amino acid residues. The pose selected was further subject to energy

minimization using Amber10:EHT forcefield at a RMS gradient of 0.1 kcal/mol/ $Å^2$.

The selected pose in complex with the respective protein was imported into the workspace of Biovia Discovery Studio Visualizer 2021, for visualization and generation of the interaction diagrams [48].

### Statistical analysis

The results were expressed as means of three independent tests ± standard deviation (SD). Statistical analysis was performed using GraphPad Prism software (version 5). One-way analysis of variance (ANOVA) was used for analysis of the experimental data considering $P < 0.05$ for significance.

## Supplementary Information

The online version contains supplementary material available at https://doi.org/10.1186/s12934-024-02421-1.

Supplementary Material 1.

**Acknowledgements**
Our gratitude goes to the Pharmacognosy laboratory at Faculdade de Ciências Farmacêuticas de Ribeirão Preto da Universidade de São Paulo (FCFRP-USP), as well as the Sao Paulo Research Foundation (2011/13630-7), both located in Brazil.

**Author contributions**
L.A., M.A., J.B., R.E. and S.A. conceived and designed the experiments. L.A., M.A., R.E. and S.A. performed the experiments. S.A. carried out the docking analysis. L.A., M.A., S.A., and R.E. analyzed the data and wrote the original draft. All authors reviewed, edited, and approved the manuscript.

**Funding**
No fund was received from any funding agency.

**Data availability**
The raw data supporting the conclusions of this article will be made available by the authors, without undue reservation, to any qualified researcher.

## Declarations

**Ethics approval and consent to participate**
Not applicable.

**Consent for publication**
Not applicable.

**Competing interests**
The authors confirm the absence of competing interests.

**Author details**
[1]Department of Microbiology and Immunology, Faculty of Pharmacy, Tanta University, Tanta, Egypt. [2]Department of Pharmacognosy, Faculty of Pharmacy, Delta University for Science and Technology, International Coastal Road, Gamasa 11152, Egypt. [3]School of Pharmacy and Biomolecular Sciences, Royal College of Surgeons in Ireland, Dublin D02 VN51, Ireland. [4]Department of Pharmaceutical Sciences, School of Pharmaceutical Sciences of Ribeirão Preto, University of São Paulo, São Paulo, SP 14040-903, Brazil. [5]Department of Pharmaceutical Chemistry, Faculty of Pharmacy, Tanta University, Tanta, Egypt. [6]Department of Microbiology and Immunology, Faculty of Pharmacy, Delta University for Science and Technology, International Coastal Road, Gamasa 11152, Egypt.

Received: 6 March 2024 Accepted: 11 May 2024
Published: 8 August 2024

**References**

1. Pitout JDD, Peirano G, Kock MM, Strydom KA, Matsumura Y. The global ascendency of OXA-48-Type carbapenemases. Clin Microbiol Rev. 2019;33(1):e00102-e119. https://doi.org/10.1128/CMR.00102-19.
2. Ambler RP. The structure of beta-lactamases. Philos Trans R Soc Lond B Biol Sci. 1980;289(1036):321–31. https://doi.org/10.1098/rstb.1980.0049.
3. Bush K, Jacoby GA. Updated functional classification of beta-lactamases. Antimicrob Agents Chemother. 2010;54(3):969–76. https://doi.org/10.1128/AAC.01009-09.
4. Bush K, Bradford PA. Epidemiology of β-lactamase-producing pathogens. Clin Microbiol Rev. 2020;33(2):e00047-e119. https://doi.org/10.1128/CMR.00047-19.
5. Cruz-López F, Martínez-Meléndez A, Morfin-Otero R, Rodriguez-Noriega E, Maldonado-Garza HJ, Garza-González E. Efficacy and in vitro activity of novel antibiotics for infections with carbapenem-resistant gram-negative pathogens. Front Cell Infect Microbiol. 2022;12:884365. https://doi.org/10.3389/fcimb.2022.884365.
6. Codjoe FS, Donkor ES. Carbapenem resistance: a review. Med Sci. 2017;6(1):1. https://doi.org/10.3390/medsci6010001.
7. Carcione D, Siracusa C, Sulejmani A, Leoni V, Intra J. Old and new beta-lactamase inhibitors: molecular structure, mechanism of action, and clinical use. Antibiotics. 2021;10(8):995. https://doi.org/10.3390/antibiotics10080995.
8. Saleem M, Rashid F, Liaqat I, Liaqat I, Ulfat M, Sultan A, Faiz M, Eijaz S, Bibi A. Phenotypic and molecular characterization of CTX-M Type B-lactamases in gram negative bacterial strains isolated from hospitals, Lahore Pakistan. J Oleo Sci. 2022;71(6):875–9. https://doi.org/10.5650/jos.ess22041.
9. Mehta SC, Furey IM, Pemberton OA, Boragine DM, Chen Y, Palzkill T. KPC-2 β-lactamase enables carbapenem antibiotic resistance through fast deacylation of the covalent intermediate. J Biol Chem. 2021;296:100155. https://doi.org/10.1074/jbc.RA120.015050.
10. Palacios-Baena ZR, Giannella M, Manissero D, Rodríguez-Baño J, Viale P, Lopes S, Wilson K, McCool R, Longshaw C. Risk factors for carbapenem-resistant Gram-negative bacterial infections: a systematic review. Clin Microbiol Infect. 2021;27(2):228–35. https://doi.org/10.1016/j.cmi.2020.10.016.
11. Aung AH, Kanagasabai K, Koh J, Hon PY, Ang B, Lye D, Chen SL, Chow A. Epidemiology and transmission of carbapenemase-producing *Enterobacteriaceae* in a health care network of an acute-care hospital and its affiliated intermediate- and long-term-care facilities in Singapore. Antimicrob Agents Chemother. 2021;65(8): e0258420. https://doi.org/10.1128/AAC.02584-20.
12. Lomovskaya O, Tsivkovski R, Nelson K, Rubio-Aparicio D, Sun D, Totrov M, Dudley MN. Spectrum of beta-lactamase inhibition by the cyclic boronate QPX7728, an Ultrabroad-spectrum beta-lactamase inhibitor of serine and metallo-beta-lactamases: enhancement of activity of multiple antibiotics against isogenic strains expressing single beta-lactamases. Antimicrob Agents Chemother. 2020;64(6):e00212-e220. https://doi.org/10.1128/AAC.00212-20.
13. Abd El-Salam M, Furtado N, Haskic Z, Lieske J, Bastos J. Antiurolithic activity and biotransformation of galloylquinic acids by *Aspergillus alliaceus* ATCC10060, *Aspergillus brasiliensis ATCC 16404, and Cunninghamella elegans* ATCC10028b. Biocatal Agric Biotechnol. 2019;18:101012. https://doi.org/10.1016/j.bcab.2019.01.050.
14. Zhao W-H, Hu Z-Q, Hara Y, Shimamura T. Inhibition of penicillinase by epigallocatechin gallate resulting in restoration of antibacterial activity of penicillin against penicillinase-producing *Staphylococcus aureus*. Antimicrob Agents Chemother. 2002;46:2266–8.
15. Qin W, Wang Y, Mouhamed F, Hamaker B, Zhang G. Impact of the solubility of phenolic compounds from highland barley (Hordeum vulgare L.) on their antioxidant property and protein binding affinity. LWT. 2023;186:115251.
16. Jiamboonsri P, Eurtivong C, Wanwong S. Assessing the Potential of gallic acid and methyl gallate to enhance the efficacy of β-lactam

antibiotics against methicillin-resistant *Staphylococcus aureus* by targeting β-lactamase: in silico and in vitro studies. Antibiotics. 2023;12:1622. https://doi.org/10.3390/antibiotics12111622.
17. Faheem M, Rehman MT, Danishuddin M, Khan AU. Biochemical characterization of CTX-M-15 from *Enterobacter cloacae* and designing a novel non-β-lactam-β-lactamase inhibitor. PLoS ONE. 2013;8(2): e56926. https://doi.org/10.1371/journal.pone.0056926.
18. Bennett PM, Chopra I. Essack Molecular basis of beta-lactamase induction in bacteria. Antimicrob Agents Chemother. 1993;37(2):153–8. https://doi.org/10.1128/AAC.37.2.153.
19. Essack SY. The development of beta-lactam antibiotics in response to the evolution of beta-lactamases. Pharm Res. 2001;18(10):1391–9. https://doi.org/10.1023/a:1012272403776.
20. Li XZ, Nikaido H. Efflux-mediated drug resistance in bacteria. Drugs. 2004;64(2):159–204. https://doi.org/10.2165/00003495-200464020-00004.
21. Thiolas A, Bornet C, Davin-Régli A, Pagès JM, Bollet C. Resistance to imipenem, cefepime, and cefpirome associated with mutation in Omp36 osmoporin of *Enterobacter aerogenes*. Biochem Biophys Res Commun. 2004;317(3):851–6. https://doi.org/10.1016/j.bbrc.2004.03.130.
22. Tondi D, Morandi F, Bonnet R, Costi MP, Shoichet BK. Structure-based optimization of a non-beta-lactam lead results in inhibitors that do not up-regulate beta-lactamase expression in cell culture. J Am Chem Soc. 2005;127(13):4632–9. https://doi.org/10.1021/ja042984o.
23. Bonnet R. Growing group of extended-spectrum beta-lactamases: the CTX-M enzymes. Antimicrob Agents Chemother. 2004;48(1):1–14. https://doi.org/10.1128/AAC.48.1.1-14.2004.
24. Mahazu S, Sato W, Ayibieke A, Prah I, Hayashi T, Suzuki T, Iwanaga S, Ablordey A, Saito R. Insights and genetic features of extended-spectrum beta-lactamase producing *Escherichia coli* isolates from two hospitals in Ghana. Sci Rep. 2022;12(1):1843. https://doi.org/10.1038/s41598-022-05869-6.
25. Galdadas I, Lovera S, Pérez-Hernández G, Barnes MD, Healy J, Afsharikho H, Woodford N, Bonomo RA, Gervasio FL, Haider S. Defining the architecture of KPC-2 Carbapenemase: identifying allosteric networks to fight antibiotics resistance. Sci Rep. 2018;8(1):12916. https://doi.org/10.1038/s41598-018-31176-0.
26. Khan A, Faheem M, Danishuddin M, Khan AU. Evaluation of inhibitory action of novel non β-lactam inhibitor against *Klebsiella pneumoniae* carbapenemase (KPC-2). PLoS ONE. 2014;9(9): e108246. https://doi.org/10.1371/journal.pone.0108246.
27. Al-Madboly LA, Abd El-Salam MA, Bastos JK, El-Shorbagy SH, El-Morsi RM. Novel preclinical study of galloylquinic acid compounds from *Copaifera lucens* with potent antifungal activity against vaginal candidiasis induced in a murine model via multitarget modes of action. Microbiol Spectr. 2022;10(5): e0272421. https://doi.org/10.1128/spectrum.02724-21.
28. Barnes MD, Winkler ML, Taracila MA, Page MG, Desarbre E, Kreiswirth BN, Shields RK, Nguyen MH, Clancy C, Spellberg B, Papp-Wallace KM, Bonomo RA. *Klebsiella pneumoniae* Carbapenemase-2 (KPC-2), substitutions at ambler position Asp179, and resistance to ceftazidime-Avibactam: unique antibiotic-resistant phenotypes emerge from β-lactamase protein engineering. MBio. 2017;8(5):e00528-e617. https://doi.org/10.1128/mBio.00528-17.
29. Abd El-Salam MA, El-Tanbouly GS, Bastos JK, Metwaly HA. Novel antitumor activity of the combined treatment of galloylquinic acid compounds with doxorubicin in solid Ehrlich carcinoma model via the Notch signaling pathway modulation. Life Sci. 2022;299:120497. https://doi.org/10.1016/j.lfs.2022.120497.
30. Abdelaziz AA, Abo-Kamer AM, Nosair AM, Al-Madboly LA. Exploring the potential efficacy of phage therapy for biocontrol of foodborne pathogenic extensively drug-resistant *Escherichia coli* in gastrointestinal tract of rat model. Life Sci. 2023;315:121362. https://doi.org/10.1016/j.lfs.2022.121362.
31. Al-Madboly LA, Abdelaziz AA, Abo-Kamer AM, Nosair AM, Abdelkader K. characterization and genomic analysis of Novel bacteriophage NK 20 to revert colistin resistance and combat pandrug resistant *Klebsiella pneumoniae* in rat respiratory infection model. Life Sci. 2023;322:121639. https://doi.org/10.1016/j.lfs.2023.121239.
32. The European Committee on Antimicrobial Susceptibility Testing. Breakpoint tables for interpretation of MICs and zone diameters. Version 14.0, 2024. http://www.eucast.org."
33. Shoeib NA, Al-Madboly LA, Ragab AE. *In vitro* and *in silico* β-lactamase inhibitory properties and phytochemical profile of *Ocimum basilicum* cultivated in central delta of Egypt. Pharm Biol. 2022;60(1):1969–80. https://doi.org/10.1080/13880209.2022.2127791.
34. Everaert A, Coenye T. Effect of β-Lactamase inhibitors on in vitro activity of β-Lactam antibiotics against *Burkholderia cepacia* complex species. Antimicrob Resist Infect Control. 2016;16(5):44. https://doi.org/10.1186/s13756-016-0142-3.
35. Ribeiro AS, Silva DA, Silva FP, Santos GC, Campos LMS, Oliveira LVN, Santos DA. Epidemiology and phospholipase activity of oral Candida spp. among patients with central nervous system diseases before and after dental cleaning procedure. Braz J Microbiol. 2010;41:19–23. https://doi.org/10.1590/S1517-83822010000100004.
36. Zhou Y, Wang T, Guo Y, Liu S, Wang J, Shen Y, Tang S, Wang Y, Deng X. *In Vitro/Vivo* activity of potential MCR-1 inhibitor in combination with colistin against*s mcr*-1-Positive *Klebsiella pneumonia*. Front Microbiol. 2018;9:1615. https://doi.org/10.3389/fmicb.2018.01615.
37. Al-Madboly LA. A novel triple combination to combat serious infections with carbapenem-resistant *Acinetobacter baumannii* in a mouse pneumonia model. Microbiol Spectr. 2022;10(5): e0271021. https://doi.org/10.1128/spectrum.02710-21.
38. Lagerbäck P, Khine WW, Giske CG, Tängdén T. Evaluation of antibacterial activities of colistin, rifampicin and meropenem combinations against NDM-1-producing *Klebsiella pneumoniae* in 24 h in vitro time-kill experiments. J Antimicrob Chemother. 2016;71(8):2321–5. https://doi.org/10.1093/jac/dkw213.
39. Yang Y, Guo Y, Zhou Y, Gao Y, Wang X, Wang J, Niu X. Discovery of a novel natural allosteric inhibitor that targets NDM-1 against *Escherichia coli*. Front Pharmacol. 2020;11:581001. https://doi.org/10.3389/fphar.2020.581001.
40. Hanes MS, Jude KM, Berger JM, Bonomo RA, Handel TM. Structural and biochemical characterization of the interaction between KPC-2 beta-lactamase and beta-lactamase inhibitor protein. Biochemistry. 2009;48(39):9185–93. https://doi.org/10.1021/bi9007963.
41. Paukner S, Hesse L, Prez˙elj A, olmajer T., UrlebU,. In vitro activity of lk-157, a novel tricyclic carbapenem as broad-spectrum _-lactamase inhibitor. Antimicrob Agents Chemother. 2009;53:505–11.
42. Poirel L, Naas T, Nicolas D, Collet L, Bellais S, Cavallo JD, Nordmann P. Characterization of VIM-2, a carbapenem-hydrolyzing metallo-beta-lactamase and its plasmid- and integron-borne gene from a Pseudomonas aeruginosa clinical isolate in France. Antimicrob Agents Chemother. 2000;44(4):891–7. https://doi.org/10.1128/AAC.44.4.891-897.2000.
43. Clifford MN, Stoupi S, Kuhnert N. Profiling and characterization by LC-MSn of the galloylquinic acids of green tea, tara tannin, and tannic acid. J Agric Food Chem. 2007;55(8):2797–807. https://doi.org/10.1021/jf063533l.
44. Kondo K, Takaishi Y, Shibata H, Higuti T. ILSMRs (intensifier of beta-lactam-susceptibility in methicillin-resistant Staphylococcus aureus) from Tara [Caesalpinia spinosa (Molina) Kuntze]. Phytomedicine. 2006;13(3):209–12. https://doi.org/10.1016/j.phymed.2004.08.001.
45. Aboukhatwa SM, Sidhom PA, Angeli A, Supuran CT, Tawfik HO. Terminators or guardians? Design, synthesis, and cytotoxicity profiling of Chalcone-Sulfonamide hybrids. ACS Omega. 2023;8(8):7666–83.
46. Aboukhatwa SM, Ibrahim AO, Aoyama H, Al-Behery AS, Shaldam MA, El-Ashmawy G, Tawfik HO. Nicotinonitrile-derived apoptotic inducers: design, synthesis, X-ray crystal structure and Pim kinase inhibition. Bioorg Chem. 2022;129:106126. https://doi.org/10.1016/j.bioorg.2022.106126
47. **ULC, C. C. G.** Molecular Operating Environment (MOE), 2020.09, 1010 Sherbooke St. West, Suite #910, Montreal, QC, Canada, H3A 2R7., 2022.
48. Dassault Systèmes BIOVIA. Discovery studio visualizer, release 2021. San Diego: Dassault Systèmes; 2021.
49. Cahill ST, Cain R, Wang DY, Lohans CT, Wareham DW, Oswin HP, Mohammed J, Spencer J, Fishwick CW, McDonough MA, Schofield CJ, Brem J. Cyclic boronates inhibit all classes of beta-lactamases. Antimicrob Agents Chemother. 2017;61(4):10.
50. Tooke CL, Hinchliffe P, Lang PA, Mulholland AJ, Brem J, Schofield CJ, Spencer J. Molecular basis of class A β-lactamase inhibition by relebactam. Antimicrob Agents Chemother. 2019;63(10):e00564-e619. https://doi.org/10.1128/AAC.00564-19.
51. Halgren TA. Merck molecular force field. I. basis, form, scope, parameterization, and performance of MMFF94. J Comput Chem. 1996;17:490–519.

52. Corbeil CR, Williams CI, Labute P. Variability in docking success rates due to dataset preparation. J Comput Aided Mol Des. 2012;26(6):775–86. https://doi.org/10.1007/s10822-012-9570-1.

## Publisher's Note